Conference Proceedings

Solar World Congress 2015
Daegu, Korea, 08 – 12 November 2015

Analysis of solar still with nanoparticle incorporated phase change material for solar desalination application

D.Dsilva Winfred Rufuss [a], S.Iniyan[a*], L.Suganthi [b], P.A.Davies[c], Takeshi Akinaga[c]
[a] Dept. of Mechanical Engineering, Anna University, Chennai 600 025, India
[b] Department of management studies, Anna University, Chennai 600025, India
[c] School of Engineering and Applied Science, Aston University, UK
dsilva.kongu@gmail.com, iniyan777@hotmail.com [*] , suganthi2764@yahoo.com,
p.a.davies@aston.ac.uk , t.akinaga@aston.ac.uk

Abstract

In the present scenario, heat storage system started to play its role in every field including solar thermal applications. This paper mainly deals with the application of heat storage medium in solar desalination still applications. This research concerns with the theoretical analysis of latent heat energy storage with the incorporation of nano particles. In this research, paraffin wax is selected as the phase change material with 0.3 weight% of nano particles such as TiO_2, CuO and Graphene Oxide. It is found that Graphene Oxide with paraffin gives the higher results comparing with the other nano particles. The thermal conductivity increased to 0.8 W/mK for Graphene Oxide nano composite and the predicted results shows that the productivity is quite high for paraffin wax with Graphene Oxide. Mathematical modeling was carried out and the results indicate that the solar still with phase change material incorporated with nano particles gives higher results than the conventional solar stills and Graphene oxide with paraffin is found to be the best nano particle for solar desalination still application. So it is best to incorporate Graphene oxide nano particle with paraffin for the experimental setup to achieve higher productivity than conventional one.

.

Keywords: Solar still, Nano particles, latent heat energy storage, paraffin, productivity

1. Introduction

Water scarcity is a major issue that affects the world. By the year 2025, it is estimated that 1.8 billion people will be affected by water scarcity, and 2/3 of the world will experience water-stressed conditions, eventually 1/2 of the world will experience high water stress by the year 2030 (72% people will be in water stress). Presently, African regions are experiencing high water stress up to 31 %, followed by Asia, America and Europe with 25%, 7% and 2% of water stress respectively [2][3][4]. Desalination has a growing role to play in meeting the demands for fresh water.

There are various methods of desalinating sea- and brackish water. The methods includes distillation, ion exchange, membrane distillation, freezing desalination, geo-thermal desalination, solar desalination, methane hydrate crystallization, high grade water recycling, and seawater greenhouse technology [5]. The energy for desalination can be obtained from fossil fuel or alternate energy sources. Among various methods of solar desalination, solar desalination using solar stills has several advantages including simplicity, economic, ease of maintenance, and low environmental impact. However, it also disadvantages, in particular low productivity, hindering the commercial uptake of desalination based on solar stills.

In single slope solar still with heat storage, there will be heat energy storage material for absorbing and storing the heat during the peak sunshine hours and it will emit the absorbed heat when the radiation decreases, such that the temperature will be maintained inside the system. Rahim formulated a method to store the heat energy in horizontal solar desalination still. It is about 47.2% efficient during nocturnal period and no external source is required to store and recover heat [6]. Salah et al predicted the thermal performance of solar still with various absorbing materials such as coated and uncoated wiry and found that uncoated sponge has highest water collection rate [7].

doi:10.18086/swc.2015.10.44 Available at http://proceedings.ises.org

Omar et al conducted the experiment in solar still with energy storage material beneath the basin and inferred that it enhances both the productivity and efficiency of the still. It is also found that melting point of phase change material also plays a vital role in productivity yield at night [8]. Dsilva et al conducted the experiment in single slope single basin solar still with roof heat and fornd that the system gives productivity till 8 o clock in the night [9]. The incorporation of TiO_2 Nano particles with stearic acid phase change material by Harikrishnan et al, the result ended with the findings that, thermal stability and thermal conductivity of phase change material is increased with the incorporation of Nano particle [10] [11]. Additionally the research is extended to the incorporation of CuO - Nano particle with Oleic acid for cooling application and ended with the findings of improvement in cooling properties [12] [13].
The inclination angle of the glass affects the parameters such as yield rate, instantaneous efficiency. Different researchers, however, reached different conclusions about the optimal inclination. Tiwari et al made an analysis by varying inclination angle for condensing cover and also done thermal modelling of passive type solar still. It is inferred that in general, 15^o inclination angle provides maximum yield rate compared with other inclination angle. [14].Muhammed et al designed a single basin solar still for south western arid region of Pakistan and concluded that the optimum glass cover angle is 33.3 ^{o} for Islamabad [15]. Rahul Dev et al conducted experiments in solar desalination still with various inclination angles for attaining the maximum instantaneous efficiency and validated the experimental observation with modelled equation and he found that the inclination angle with 45^0 gives the maximum instantaneous efficiency [16].
The double basin solar still gives more productivity during the cooling period whereas single basin solar still gives more productivity during heating period. Elango et al performed an experiment to analyse the relation between water depth and productivity in double basin solar still. The result ends with the conclusion that double basin solar still yields more distillate only when the water depth is maintained at 1 cm [17].Hitesh conducted the experiment in double basin solar still with vacuum tube and black gravel granite attached to it. The result infers that when the still is coupled with vacuum tube and granite, the system gives higher productivity, than they are coupled individually [18]. The listed literature are some of the passive type solar stills, the active type solar stills includes the addition of collector, concentrator, air heaters, condensers etc.

The use of a collector increases the heat input to the still; therefore it may also be necessary to enhance the heat output to achieve condensation. This has been done using a humidifying tower and condensing cover. Farhad et al analysed exergy and energy for solar desalination system with a flat-plate solar collector by both experimentally and theoretically and found that there was a decrease in exergy efficiency by increasing the length of the humidification tower and that the exergy efficiency increased with decrease in inlet air temperature and tower diameter [19].Dimri conducted an experiment with effect of condensing cover with the yield of active solar still and inferred that productivity was directly proportional to the thermal conductivity of material ofthe condensing cover. Thus copper results in greater yield compared to glass and plastic since it has higher thermal conductivity [20].Tiwari et al made an analysis to relate instantaneous thermal efficiency and collector area. In this research the energy balance for each component was considered and the research ended with the formulation of equations for the various components of the still [21]. The coupling of an air heater to the solar still increased the water temperature in the basin and thus promoted the evaporation rate. Sampathkumar et al carried out a study on various active solar stillsand found that the air heater increased productivity by up to 70% [22]. This productivity is high compared with that of stills coupled with flat plate collectors, evacuated tube collectors and concentrators. Various design modifications such as heat storage, and water spraying have been done on solar stills, with air heater to achieve higher productivity. To investigate the effect of heat storage, Abdulha performed an experiment in stepped solar still solar air heater and latent heat energy storage and discussed the method for increasing the performance by adding aluminium filling. It was found that the integration gave 53% more productivity than conventional set up [23].

In active solar stills, solar collectors can be used to boost performance – including flat plate, evacuated tube, and flat plate collectors. Solar ponds and air heaters have also been used. Air heaters are effective combined with energy storage and with water spraying arrangements.

2. Mathematical Modeling

2.1 Assumptions

A solar still utilizes the heat from the sun to heat the water inside a basin. Hence evaporation takes place and the condensate is trapped by the glass cover at the top of the basin and collected through the distillate collector. The base of the still is covered by insulating material to avoid the heat loss. The productivity is about 2–5 L/m^2.day, thus more than 1 m^2 is required to supply the needs of one person. Fig. 1 gives the pictorial representation of solar still in x-y-z coordinate where as fig. 2 represents the layer wise identification of various components of solar still namely Phase change material, water, air, glass and air layers in x-y coordinate. The whole work has been carried in Institute for Energy Studies, Anna University Chennai, India and Aston University, UK.

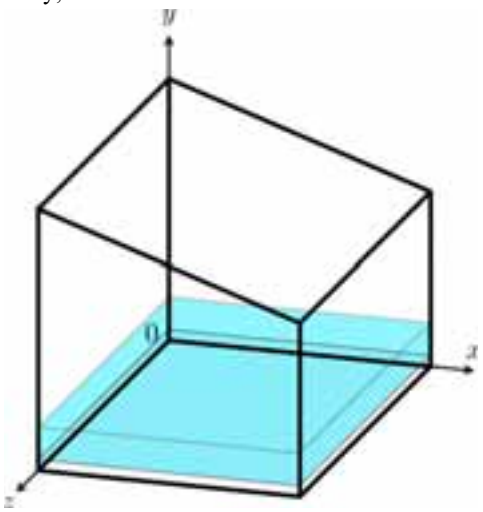

Fig. 1

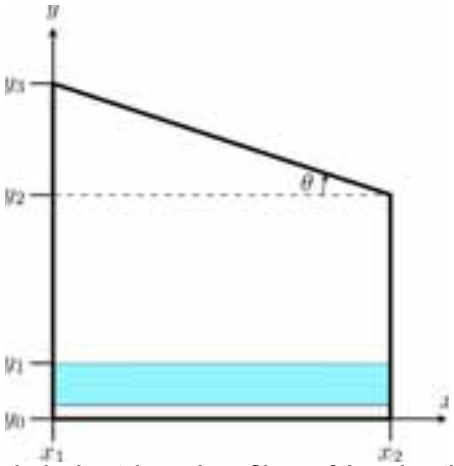

Figure 2: Solar still placed on the horizontal *z*−*x* plane. Shape of the solar still is monotonic in *z* direction.

The following assumptions are made,

a. It is assumed that the shape of the solar still is monotonic un z direction.
b. Energy input is based on only the solar energy (radiation).
c. Intensity of the solar radiation (I) and the ambient temperature (T_a) are controlling the system.
d. I changes gradually in time, I = I (tau), dI/dtau~0.
e. Temperature for water (T_w) and PCM (T_{PCM}) are same. There is no distribution for T_w and T_{PCM}, but T_w and T_{PCM} are function of time (tau). (I and T_a, implicitly, because I=I(tau) and T_a=T_a(tau)).
f. Total energy input to solar still per day, I' * area * time, yields the water production per day (via evaporation and) via condensation of water.

g. Heat capacities of basin liner and insulating material are negligible compared to those for the basin water and phase change material (PCM).
h. The system is vapour tight and the side losses are negligible.
i. PCM and basin liner are in good contact.

Using the above mentioned assumptions the mathematical modeling was carried out using vorticity transport equation, the energy equation and diffusion equation and the analysis has been conducted with respect to Chennai, India climatic condition taking the input from weather data in U.S Department of Energy. The following table represents the data taken for analysis from U.S Department of Energy.

Table.1 *IND_Chennai.432790_IWEC.stat*: Average Hourly Statistics for Global Horizontal Solar Radiation Wh/m^2.

Hours	Jan	Feb	Mar	Apr	May	Jun	Jul	Aug	Sep	Oct	Nov	Dec
0:01 – 1:00	0	0	0	0	0	0	0	0	0	0	0	0
1:01 – 2:00	0	0	0	0	0	0	0	0	0	0	0	0
2:01 – 3:00	0	0	0	0	0	0	0	0	0	0	0	0
3:01 – 4:00	0	0	0	0	0	0	0	0	0	0	0	0
4:01 – 5:00	0	0	0	0	0	0	0	0	0	0	0	0
5:01 – 6:00	0	0	0	0	1	1	0	0	0	0	0	0
6:01 – 7:00	4	6	15	40	62	58	36	26	32	29	16	9
7:01 – 8:00	96	116	176	234	251	235	179	166	200	190	147	119
8:01 – 9:00	300	350	416	446	451	424	349	337	400	375	316	303
9:01 – 10:00	497	571	647	668	649	593	498	495	577	540	471	467
10:01 – 11:00	640	732	807	836	800	710	609	616	701	656	576	572
11:01 – 12:00	707	809	873	930	887	765	669	685	765	711	616	599
12:01 – 13:00	742	862	920	963	895	775	681	709	771	709	629	616
13:01 – 14:00	703	829	875	908	830	718	633	670	704	638	571	571
14:01 – 15:00	591	713	744	772	700	599	532	571	574	508	450	464
15:01 – 16:00	420	524	559	574	510	451	407	426	412	340	291	315
16:01 – 17:00	211	291	322	329	291	269	250	248	218	153	115	137
17:01 – 18:00	34	71	90	94	88	92	93	79	47	16	9	13
18:01 – 19:00	0	1	3	3	4	7	7	4	1	0	0	0
19:01 – 20:00	0	0	0	0	0	0	0	0	0	0	0	0
20:01 – 21:00	0	0	0	0	0	0	0	0	0	0	0	0
21:01 – 22:00	0	0	0	0	0	0	0	0	0	0	0	0
22:01 – 23:00	0	0	0	0	0	0	0	0	0	0	0	0
23:01 – 24:00	0	0	0	0	0	0	0	0	0	0	0	0
Max Hour	13	13	13	13	13	13	13	13	13	12	13	13
Min Hour	1	1	1	1	1	1	1	1	1	1	1	1

2.2 Mathematical formulation

Two dimensional flow in the vertical (x-y) plane is studied for an incompressible Newtonian Boussinesq fluid. It is convenient to introduce the stream function ψ so that continuity equation is satisfied automatically, because

$$u=\frac{\partial \psi}{\partial y}, \quad v=-\frac{\partial \psi}{\partial x}. \qquad \text{(eq.1)}$$

The governing equation is the vorticity transport equation, the energy equation and diffusion equation for absolute humidity as follow:

$$\frac{\partial \omega}{\partial t} = \frac{\partial \psi}{\partial x}\frac{\partial \omega}{\partial y} - \frac{\partial \psi}{\partial y}\frac{\partial \omega}{\partial x} + \nu\left(\frac{\partial^2 \omega}{\partial x^2} + \frac{\partial \omega}{\partial y^2}\right) + \beta\frac{\partial T}{\partial x}, \quad \text{(eq.2)}$$

$$\frac{\partial T}{\partial t} = \frac{\partial \psi}{\partial x}\frac{\partial T}{\partial y} - \frac{\partial \psi}{\partial y}\frac{\partial T}{\partial x} + \frac{\lambda}{\varrho C_p}\left(\frac{\partial^2 T}{\partial x^2} + \frac{\partial T}{\partial y^2}\right), \quad \text{(eq.3)}$$

$$\frac{\partial e}{\partial t} = \frac{\partial \psi}{\partial x}\frac{\partial e}{\partial y} - \frac{\partial \psi}{\partial y}\frac{\partial e}{\partial x} + \kappa vap\left(\frac{\partial^2 e}{\partial x^2} + \frac{\partial e}{\partial y^2}\right), \quad \text{(eq.4)}$$

where z component of the vorticity (ω) is written in

$$\omega = -\left(\frac{\partial^2 \psi}{\partial x^2} + \frac{\partial \psi}{\partial y^2}\right). \quad \text{(eq.5)}$$

Transformation for general coordinates

Transformation of coordinates system: x=x(ξ,η), y=y(ξ,η).

$$\frac{\partial x}{\partial x} = \frac{1}{J}\left(\frac{\partial y}{\partial \eta}\frac{\partial x}{\partial \xi} - \frac{\partial y}{\partial \xi}\frac{\partial x}{\partial \eta}\right), \quad \frac{\partial x}{\partial y} = \frac{1}{J}\left(\frac{\partial x}{\partial \xi}\frac{\partial x}{\partial \eta} - \frac{\partial x}{\partial \eta}\frac{\partial x}{\partial \xi}\right). \quad \text{(eq.6)}$$

$$\frac{\partial^2 x}{\partial x^2} + \frac{\partial^2 x}{\partial y^2} = \frac{1}{J^2}\left(D + C_\xi\frac{\partial x}{\partial \xi} + C_\eta\frac{\partial x}{\partial \eta}\right). \quad \text{(eq.7)}$$

Herein

$$J = \frac{\partial x}{\partial \xi}\frac{\partial y}{\partial \eta} - \frac{\partial x}{\partial \eta}\frac{\partial y}{\partial \xi}, \quad C_\xi = \frac{1}{J}\left[\frac{\partial x}{\partial \eta}D(y) - \frac{\partial y}{\partial \eta}D(x)\right], \quad C_\eta = \frac{1}{J}\left[\frac{\partial y}{\partial \xi}D(x) - \frac{\partial x}{\partial \xi}D(y)\right]. \quad \text{(eq.8)}$$

A linear operator D is defined as

$$D \equiv C_{\xi\xi}\frac{\partial^2 y}{\partial \xi^2} - 2C_{\xi\eta}\frac{\partial^2 y}{\partial \xi \partial \eta} + C_{\eta\eta}\frac{\partial^2 y}{\partial \eta^2}, \quad \text{(eq.9)}$$

where

$$C_{\xi\xi} = \left(\frac{\partial x}{\partial \eta}\right)^2 + \left(\frac{\partial y}{\partial \eta}\right)^2, \quad C_{\xi\eta} = \frac{\partial x}{\partial \xi}\frac{\partial x}{\partial \eta} + \frac{\partial y}{\partial \xi}\frac{\partial y}{\partial \eta}, \quad C_{\eta\eta} = \left(\frac{\partial x}{\partial \xi}\right)^2 + \left(\frac{\partial y}{\partial \xi}\right)^2. \quad \text{(eq.10)}$$

Tetragon $(x_1,y_1) - (x_2,y_1) - (x_2,y_2) - (x_1,y_3) - (x_1,y_1)$ (Figure: 1 and 2) in physical coordinates (x,y) is transformed onto/into a square $|\xi| \le 1$ and $|\eta| \le 1$ in the computational coordinates (ξ,η):

$$x = \frac{\xi+1}{2}(x_2 - x_1) + x_1 = x(\xi), \quad \text{(eq.11)}$$

$$y = \frac{\eta+1}{2}\left[\frac{\xi+1}{2}(y_2 - y_3) + (y_3 - y_1)\right] + y_1 = y(\xi,\eta). \quad \text{(eq.12)}$$

Then,

$$\frac{\partial x}{\partial \xi} = \frac{x_2 - x_1}{2}, \quad \text{(eq.13)}$$

$$\frac{\partial y}{\partial \xi} = \frac{\eta+1}{4}(y_2 - y_3), \quad \text{(eq.14)}$$

$$\frac{\partial y}{\partial \eta} = \frac{\xi+1}{4}(y_2 - y_3) + \frac{1}{2}(y_3 - y_1), \quad \text{(eq.15)}$$

$$\frac{\partial^2 y}{\partial \xi \partial \eta} = \frac{y_2 - y_3}{4}, \quad \text{(eq.16)}$$

$$\frac{\partial x}{\partial \eta} = \frac{\partial^2 x}{\partial \xi^2} = \frac{\partial^2 x}{\partial \xi \eta} = \frac{\partial^2 x}{\partial \eta^2} = \frac{\partial^2 y}{\partial \xi^2} = \frac{\partial^2 y}{\partial \eta^2} = 0. \quad \text{(eq.17)}$$

$$\frac{\partial x}{\partial x} = \frac{1}{J}\left(\frac{\partial y}{\partial \eta}\frac{\partial x}{\partial \xi} - \frac{\partial y}{\partial \xi}\frac{\partial x}{\partial \eta}\right), \quad \text{(eq.18)}$$

$$\frac{\partial x}{\partial y} = \frac{1}{J}\left(\frac{\partial x}{\partial \xi}\frac{\partial x}{\partial \eta}\right), \quad \text{(eq.19)}$$

$$\frac{\partial^2 x}{\partial x^2} + \frac{\partial^2 x}{\partial y^2} = \frac{1}{J^2}\left(C_{\xi\xi}\frac{\partial^2 x}{\partial \xi^2} - 2C_{\xi\eta}\frac{\partial^2 x}{\partial \xi \partial \eta} + C_{\eta\eta}\frac{\partial^2 x}{\partial \eta^2} + C_{\xi}\frac{\partial x}{\partial \xi} + C_{\eta}\frac{\partial x}{\partial \eta}\right). \quad \text{(eq.20)}$$

Here,

$$J = \frac{\partial x}{\partial \xi}\frac{\partial y}{\partial \eta}, \quad \text{(eq.21)}$$

$$C_{\xi\xi} = \left(\frac{\partial y}{\partial \eta}\right)^2, \quad C_{\xi\eta} = \frac{\partial y}{\partial \xi}\frac{\partial y}{\partial \eta}, \quad C_{\eta\eta} = \left(\frac{\partial x}{\partial \xi}\right)^2 + \left(\frac{\partial y}{\partial \xi}\right)^2, \quad \text{(eq.22)}$$

$$C_{\xi} = 0, \quad C_{\eta} = \frac{1}{J}\left(-\frac{\partial x}{\partial \xi}Dy\right), \quad Dx = 0, \quad Dy = -2\beta\frac{\partial^2 y}{\partial \xi \partial \eta}. \quad \text{(eq.23)}$$

$$\frac{\partial x}{\partial \xi} = \frac{x_2 - x_1}{2}, \quad \frac{\partial x}{\partial \eta} = 0, \quad \text{(eq.24)}$$

$$\frac{\partial y}{\partial \xi} = \frac{\eta + 1}{4}\left(y_3 - y_1\right), \quad \frac{\partial y}{\partial \eta} = \frac{1}{4}\left[\xi\left(y_3 - y_1\right) + \left(-2y_1 + y_2 + y_3\right)\right], \quad \text{(eq.25)}$$

$$\frac{\partial^2 y}{\partial \xi \partial \eta} = \frac{y_3 - y_1}{4}. \quad \text{(eq.26)}$$

3. Analysis, Results and Discussion

The analyses are carried out with the codes using FORTRAN software compiler in Aston University, UK. The following results are made

The temperature profile for different layers like Phase change material (PCM), basin liner, water, air, glass, bulk are shown in figure 3 with respect to height of the still. From the figure 3, the water temperature and the basin temperature are more or less equal and the PCM temperature is found to be slightly high compared to basin temperature. Melting point of PCM plays a vital role in the selection of PCM with various applications. This gives the different melting and solidification characteristics of the PCM. Here we have incorporated Nano particles to enhance the heat transfer rate and thermal conductivity of the PCM with the insulation in side and bottom.

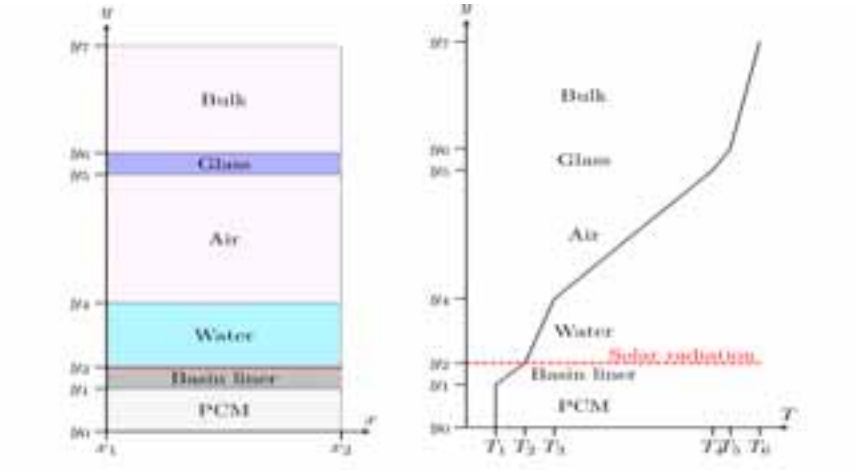

Fig : 3 Temperature profile for various layer

The work carried out with various ambient temperatures such as 20, 30, 40 C and the humidity with 0.1 and 0.2. The results for variation of water temperature and productivity with respect to solar radiation are shown in figure 4 and 5.

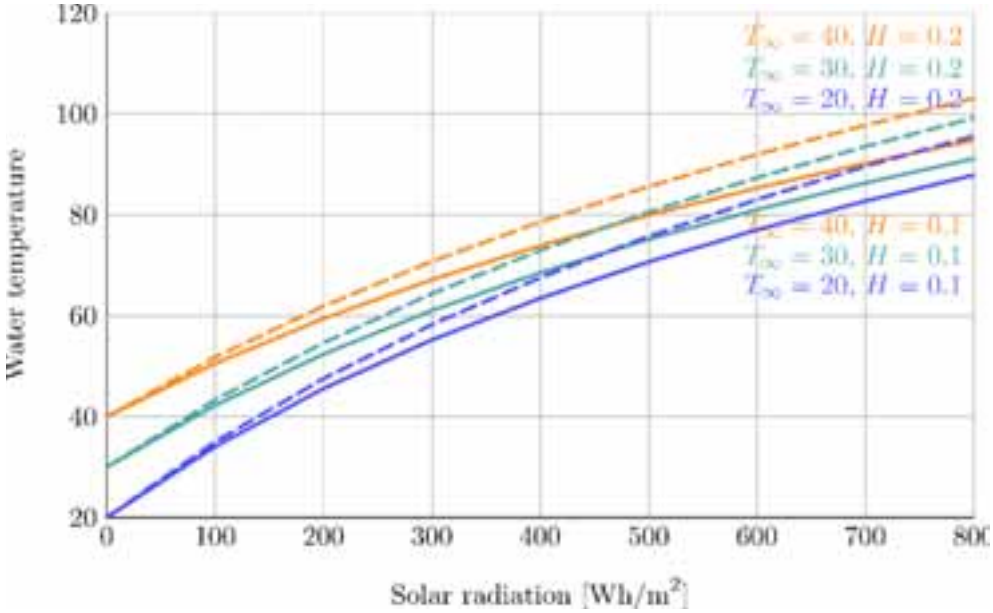

Fig:4 Water temperature Vs Solar radiation

In figure 4, the dotted line represents the water temperature variation with the relative humidity of 10% and the normal line represents the water temperature variation with the humidity of 20% and it indicates that the temperature increases with the decrease in relative humidity and decrease in moisture content. And temperature decreases with the increase in relative humidity and moisture content. From the graph, it is found that the ambient temperature and water temperature are directly proportional to each other.

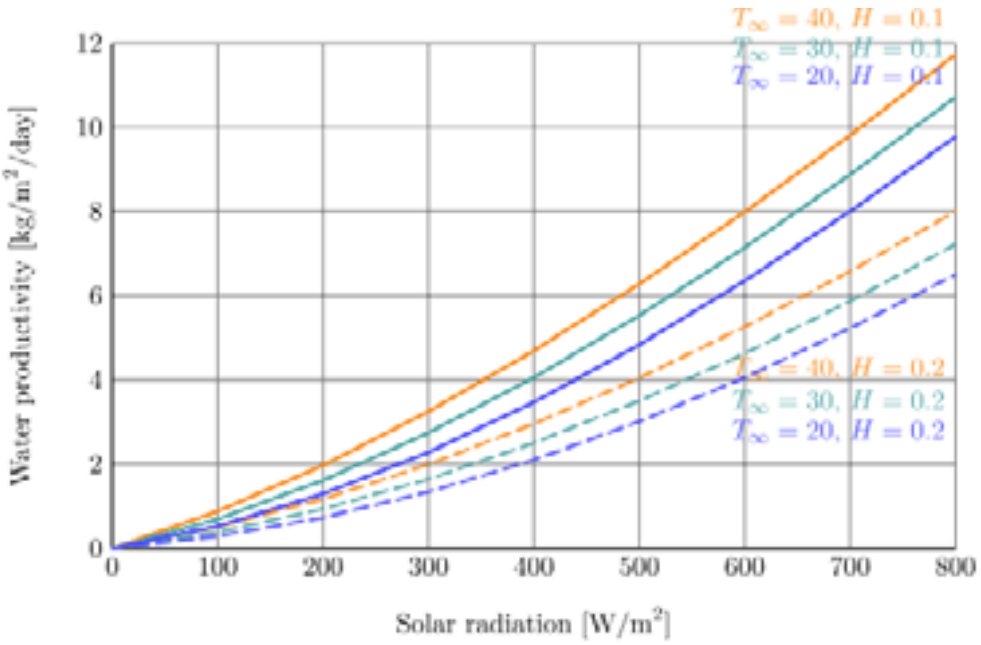

Fig .5: Water productivity Vs Solar radiation

Figure 5 represents the variation of water productivity with respect to solar radiation, Dotted line and normal line represents the variation of 10, 20% relative humidity with different ambient temperatures respectively. As the solar radiation increases, the water productivity increases gradually and there is a huge difference between 10% and 20% relative humidity. The productivity with 20% relative humidity at 40^{o}C ambient temperature was around 8 kg/m^2/day, whereas the productivity with 10% relative humidity at 40^{o}C ambient temperature was around 11.5 kg/m^2/day. The productivity is found to be comparably high for still with phase change material with nano particles, whereas the conventional still yields only 5 kg/m^2/day [9][14]. Our predicted result yields the productivity twice that of the conventional still.

From the graph, it is found that the peak productivity can be achieved during intense solar radiation, and hence the hourly productivity yield can be increased. From the single-effect and multi-effect solar stills, multi-effect solar still gives higher productivity than single-effect still. Now from the modeling result, it is quite clear that the single effect still with phase change material incorporated with nano particles yields the productivity equal to multi-effect solar still.

4. **Conclusion**.

The research aims to incorporate nano particles with phase change material for solar desalination applications. As a part, this paper provides the result of the mathematical modeling done on solar still using phase change material incorporated with nano particles. From the results, it is concluded that the addition of nano particles with phase change material enhances the productivity and the daily yield is achieved up to 12 kg/m^2/day which is quite high than the productivity of other conventional stills. So, from this paper, it is evident that the solar still using phase change materials incorporated with nano particles is superior to other conventional solar stills in all aspects. Therefore further experimental tests and optimization can be carried out as present mathematical modeling gives the concrete evidence for increased performance.

Nomenclature

A_c	Collector area, m^2
C_p	Specific heat, $Jkg^{-1}K^{-1}$
D_h	Hydraulic diameter, m
f	Friction factor, Non dimension
I	Intensity of radiation, Wm^{-2}
k	Thermal conductivity, $W\ m^{-1}K^{-1}$
k_i	Thermal conductivity of insulation material $W\ m^{-1}K^{-1}$
k_w	Thermal conductivity of the tube wall,$W\ m^{-1}K^{-1}$
L	Length of the tube, m
m	mass flow rate, kgs^{-1}
N	Number of tube, Non dimension
Nu	Nusselt number, Non dimension
Pr	Prandtl number, Non dimension
Re	Reynolds number, Non dimension
Q_{ab}	Heat absorbed, W
T_{Out}	Outlet temperature of the collector, K
T_{in}	Inlet temperature of the collector, K
T_a	Atmospheric temperature, K
V	Velocity, ms^{-1}

Greek Symbol

ρ	Density, kgm^{-3}
μ	Dynamic viscosity, Nsm^{-2}
μ_w	Dynamic viscosity of tube wall, Nsm^{-2}
η	Efficiency, %

Suffix

PT	Plain tube
RT	Rod as extended surface
TT	Tube as extended surface

Reference

[1] Kabeel A E, S.A. El-Agouz. Review of researches and developments on solar stills. Desalination 2011; 276: 1–12.

[2] Bakkes J. A. Background report to the OECD environmental Outlook to 2030: overviews, details, and methodology of model-based analysis. Netherlands Environmental Assessment Agency (MNP), 2008.

[3] Arnell N. W. Climate change and global water resources: SRES emissions and socio-economic scenarios. Global environmental change, 14(1), 31-52.

[4] Barker R, Dawe D, Tuong T. P, Bhuiyan S. I., & Guerra L. C. (1999). The outlook for water resources in the year 2020: challenges for research on water management in rice production. Southeast Asia 1999; 1: 1-5.

[5] Lourdes García-Rodríguez. Assessment of most promising developments in solar desalination. Springer 2007; Solar Desalination for the 21st Century: 355-369.

[6] Rahim N.H.A. New method to store heat energy in horizontal solar desalination still. Renewable Energy 2003; 28: 419–433.

[7] Salah Abdallah ,Mazen M. Abu-Khader , Omar Badran. Effect of various absorbing materials on the thermal performance of solar stills. Desalination 2009; 242:128-137.

[8] Omar Ansari, Mohamed Asbik, Abdallah Bah, AbdelazizArbaoui, Ahmed Khmou. Desalination of the brackish water using a passive solar still with a heat energy storage system. Desalination 2013; 324: 10–20.

[9] R.Manivel, D.Dsilva Winfred Rufuss, S.Sivakumar. Experimental Investigation of Solar Desalination System with Roof Heating. International Journal of Earth Science and Engineering 2013; 7: 1459-1464

[10] Harikrishnan S, Magesh S &Kalaiselvam S. Preparation and thermal energy storage behaviour of stearic acid–TiO 2 Nanofluids as a phase change material for solar heating systems. ThermochimicaActa 2013; 565: 137-145.

[11] Harikrishnan S &Kalaiselvam S. Preparation and thermal characteristics of CuO–oleic acid Nanofluids as a phase change material. ThermochimicaActa 2012, 533, 46-55.

[12] Mettawee E. B. S &Assassa G. M. Thermal conductivity enhancement in a latent heat storage system. Solar Energy 2007; 81(7): 839-845.

[13] Kalaiselvam S, Parameshwaran R &Harikrishnan S. Analytical and experimental investigations of Nanoparticles embedded phase change materials for cooling application in modern buildings. Renewable Energy 2012; 39(1): 375-387.

[14] Anil Kr. Tiwari and G. N. Tiwari. Annual performance analysis and thermal modelling of passive solar still for different inclinations of condensing cover. International Journal of Energy Research 2007; 31: 1358-1382.
[15] Muhammad Ali Samee, Umar K. Mirza, Tariq Majeed,Nasir Ahmad. Design and performance of a simple single basin solar still. Renewable and Sustainable Energy Reviews 2007; 11: 543–549.
[16] Rahul Dev, Tiwari G.N. Characteristic equation of a passive solar still. Desalination 2009; 245: 246–265.
[17] Elango T & Murugavel K. K. The effect of the water depth on the productivity for single and double basin double slope glass solar stills. Desalination 2015; 359: 82-91.
[18] Panchal H. N. Enhancement of distillate output of double basin solar still with vacuum tubes. Journal of King Saud University-Engineering Sciences 2013.
[19] FarhadNematollahi, Amir Rahimi, TourajTavakoliGheinani. Experimental and theoretical energy and exergy analysis for a solar desalination system. Desalination 2013; 317: 23–31.
[20] Vimal Dimri, Bikash Sarkar, Usha Singh, G.N.Tiwari. Effect of condensing cover material on yield of an active solar still: an experimental validation. Desalination 2008; 227: 178–189.
[21] Tiwari G.N, Sandy Kumar, Sharma P.B, Emran Khan M. Instantaneous thermal efficiency of an active solar still. Applied Thermal Engineering 1996; 16: 189-192.
[22] Sampathkumar K, Senthilkumar P. Utilization of solar water heater in a single basin solar still—an experimental study. Desalination 2012; 297: 8–19.
[23] Abdullah A.S. Improving the performance of stepped solar still. Desalination 2013; 319: 60–65.